

Engineering bound state in continuum via giant atom in photonic waveguide

Xiaojun Zhang,¹ Mingjie Zhu,¹ and Zhihai Wang^{1,*}

¹Center for Quantum Sciences and School of Physics,
Northeast Normal University, Changchun 130024, China

The bound state in the continuum (BIC) in photonic system has been widely used in the field of lasing and sensing. We here find the controllable BIC in an artificial giant atom-dressed one-dimensional photonic waveguide. The giant atom couples to the waveguide via two distant sites. We find that the energy and the photonic distribution in the BIC can be controlled on demand by tuning the frequency and the size of the giant atom as well as its coupling phase with the waveguide. More interestingly, we predict the quantum beats in the atomic and photonic dynamical evolution, which is induced by the oscillation between the BIC and bound state outside the continuum (BOC). These findings provide an approach to manipulate the waveguide system via the bound states, and can be applied in the quantum information processing.

I. INTRODUCTION

The bound state in the continuum (BIC) is a kind of peculiar states, which are remain localized even though it resides in the radiation continuum [1–3]. With the assistance of the BIC in photonic system, the light-matter interaction can be significantly enhanced [4, 5]. Therefore, the BIC is nowadays used to generate low threshold laser [6–8], enhance the nonlinear responds [9, 10], realize the quantum sensing [11, 12] and high efficient wave guiding [13–16], etc.

The waveguide provides the channel for photons traveling in the confined structure. Meanwhile, the waveguide also serves as a data bus, to induce the coherent interaction and incoherent collective dissipation between quantum emitters. In Ref. [17], the authors revealed that BIC can avoid the adverse effects of environment on quantum information processing, and proposed a feasible experimental scheme to realize BIC.

In the traditional waveguide community, the atom or artificial atom was usually considered as point like dipole. However, in 2014, the coherent coupling between the superconducting transmon qubit and the surface acoustic waves [18] break down the dipole approximation. In this setup, the size of the transmon is in the same order of the acoustic wavelength, and one has to consider the effects of non-local coupling via multiple points, leading to giant atom quantum optics. Subsequently, the giant atom setup was realized by coupling the transmon or magnon spin ensemble to the curved transmission line and proposed in the synthesis dimension domain [19–22]. The interference and retardation effect due to the non-local coupling in the giant atom system has evoked lots of attentions theoretically to demonstrate some exotic phenomena, such as non-Markovian oscillation [23, 24], decoherence-free interaction [25, 26], retardation effect [27, 28], Lamb shift [29] and chiral photonic population [30–32]. The combination of the the topological photons and the giant atom also induces some inter-

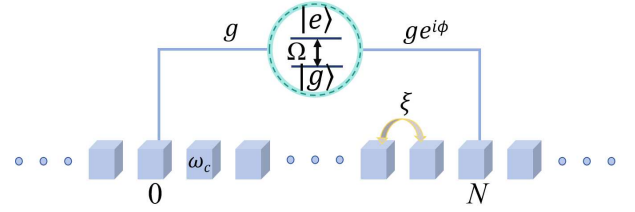


FIG. 1. Sketch of the waveguide QED setup, where a giant atom is coupled to a coupled resonator waveguide via the 0th and the Nth sites.

esting effects, for example the chiral zero mode [27, 33], the vacuum like dressed states [34], the wide band photonic reflection [35].

Recently, people have found that the BIC can exist in the giant atom-waveguide coupling system, where the waveguide is characterized by the linear or cosine type dispersion relation [36–38]. The underlying physics under the BIC generation is such giant atom is decoupled from the waveguide due to the destructive interference effect. Once the condition of the BIC is fulfilled, we can obtain the persistent oscillation without dissipation. Moreover, a controllable magic cavity QED system is also simulated under the BIC physics [38]. Since a controllability quantum system is necessary in quantum information processing, how to control the BIC in the giant atom scenario is deserved to investigated in detail.

In this paper, we promote a scheme to realize the BIC manipulation by coupling a giant atom to the coupled resonator waveguide via two sites non-locally. We analytically obtain the photonic distribution for the BIC. Moreover, we find that both of the BIC and bound states out of continuum (BOC) participate the dynamics of the system, and the BIC-BOC oscillation leads to the exotic quantum beat, which does not exist in the tradition small atom setup.

* wangzh761@nenu.edu.cn

II. MODEL

As schematically shown in Fig. 1, a single giant atom is coupled with the CRW via the 0th and N th sites. The Hamiltonian of the structure in real space reads $H = H_A + H_c + H_I$ where ($\hbar = 1$)

$$H_A = \Omega|e\rangle\langle e|, \quad (1)$$

$$H_c = \omega_c \sum_j a_j^\dagger a_j - \xi \sum_j (a_{j+1}^\dagger a_j + a_j^\dagger a_{j+1}), \quad (2)$$

$$H_I = g[(a_0^\dagger + a_N^\dagger e^{i\phi})\sigma_- + \text{H.c.}]. \quad (3)$$

Here, H_A and H_c are the Hamiltonian of the GA and the CRW respectively and H_I represents their interaction. Here we have neglected the counter-rotating terms and performed the dipole approximation at each coupling point between the GA and the CRW. Ω is the transition frequency of the GA between the ground state $|g\rangle$ and the excited state $|e\rangle$. ω_c is the intrinsic frequency of each resonator in the CRW. a_j is the annihilation operator of the j th resonator in the CRW, $\sigma_+ = |e\rangle\langle g|$ is the raising operator of the GA. ξ is the hopping strength between the nearest resonators in CRW. g is the real coupling strength between the GA and the connected resonator. We have assumed that the coupling phase in the left leg is zero while that for the right leg is ϕ .

We consider that the CRW is composed by infinite resonators so that the waveguide satisfies the translation invariance. By the Fourier transformation $a_k^\dagger = \sum_j a_j^\dagger \exp(-ikj)/\sqrt{N_c}$ with $N_c \rightarrow \infty$ being the length of the waveguide, the Hamiltonian of CRW H_c is expressed as $H_c = \sum_k \omega_k a_k^\dagger a_k$ where the dispersion relation satisfies $\omega_k = \omega_c - 2\xi \cos k$. It describes that the single photon energy band is centered at ω_c and posses a width of 4ξ . In term of the operator a_k , the interaction Hamiltonian becomes

$$H_I = \frac{g}{\sqrt{N_c}} \sum_k [a_k^\dagger \sigma_- (1 + e^{i(kN+\phi)}) + \text{H.c.}], \quad (4)$$

$N_c \rightarrow \infty$ is the length of CRW. It is obvious that the coupling amplitude between the GA and its resonant mode in the CRW is

$$G(\phi) = \frac{g}{\sqrt{N_c}} (1 + e^{i(KN+\phi)}) \quad (5)$$

which is ϕ dependent and K satisfies $\Omega = \omega_c - 2\xi \cos K$.

III. MODULATION OF THE BIC

In Figs. 2(a) and (c), we numerically plot the energy spectrum of system in the single excitation subspace for different atomic resonant frequency and coupling phase ϕ . As expected, in both of the parameter conditions, we find a pair of bound states which locate above and below the continual band respectively. In what follows, we name them as bound states out of continuum

(BOC). These BOCs originate from the broken of the translational symmetry of the waveguide induced by the GA. Not only in the GA setup, the BOCs also exist in the CRW system which couples to the traditional small atom(s) [39–41].

In the continual band, we also observe a bound state when the condition $|G(\phi)|^2 = 0$ is satisfied [37], this is the so called BIC [38]. The underlying physics is that the GA is decoupled from the resonant mode in the waveguide. However, the rest off resonant modes contributes and the BIC is still the atom-photon dressed state.

To further investigate the character of the BIC, we resort to the single photon wave function ansatz of

$$|\phi\rangle = \alpha\sigma_+|G\rangle + \sum_k \beta_k a_k^\dagger |G\rangle, \quad (6)$$

where $|G\rangle$ represents that both of the GA and the waveguide are in their ground state. According to the Schrödinger equation $H|\phi\rangle = E|\phi\rangle$, we can get

$$E = \Omega + \frac{g^2}{\pi} \int_{-\pi}^{\pi} \frac{1 + \cos(kN + \phi)}{E - \omega_c + 2\xi \cos k} dk, \quad (7)$$

$$\frac{\beta_k}{\alpha} = \frac{1}{2\pi} \frac{[g + g e^{i(kN+\phi)}]}{E - \omega_c + 2\xi \cos k} \quad (8)$$

and the photon distribution in the real space reads

$$\beta_j = \int_{-\pi}^{\pi} \beta_k e^{-ikj} dk. \quad (9)$$

In Ref. [38], we have shown the BIC in the system when the giant atom ($N = 4m + 2, m = 0, 1, 2 \dots$) is resonant with the bare resonator in the waveguide ($\Omega = \omega_c$) by taking the coupling phase to be zero ($\phi = 0$). Moving to the non-resonant case, the energy spectra in Fig. 2 (a) and (c) illustrate that the BIC (blue line) locate at the atomic frequency Ω when the coupling phase satisfies $|G(\phi)|^2 = 0$. As proven analytically in the appendix, $E = \Omega$ is always a solution of Eq. (7) in the condition of $|G(\phi)|^2 = 0$ for arbitrary $\omega_c - 2\xi < \Omega < \omega_c + 2\xi$, which agrees with the results in Fig. 2 (a) and (c). Furthermore, we can also obtain the photonic distribution for the BIC in Figs. 2 (b) and (d). Here, the solid bar represents the numerical results which comes from the direct diagonalization of the Hamiltonian and the empty circles is the analytical results which is expressed as (see Appendix for detail)

$$\frac{\beta_j}{\alpha} = \begin{cases} 0 & , j < 0 \& j > N \\ \frac{2g \sin Kj}{\sqrt{4\xi^2 - \Delta^2}} & , 0 \leq j \leq N \end{cases} \quad (10)$$

where $\Delta = \Omega - \omega_c$ is the detuning between the giant atom and the bare frequency of the resonator in the waveguide.

Explicitly, we here find some exotic characters of the single photon BIC as shown in Figs. 2 (b) and (d). For $\Omega/\xi = -1, \phi = \pi, N = 6$, we observe a dimerised character in Fig. 2 (b). That is, the photon is bounded in

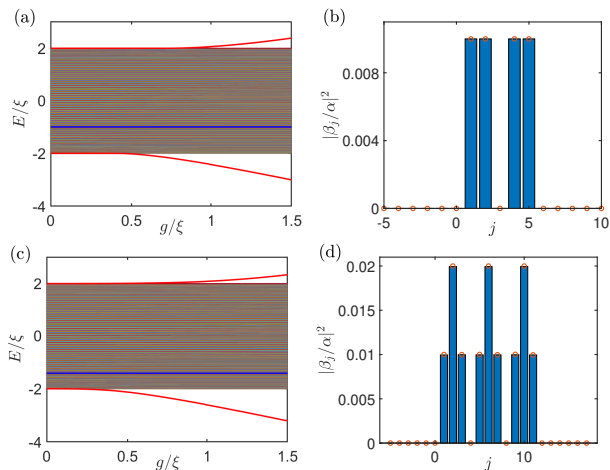


FIG. 2. (a,c) The energy diagram of the giant atom-CRW coupled system where the thick blue line in the continuum is the BIC. (b,d) The photonic distribution in the BIC. We have set $g = 0.1\xi, \omega_c = 0$. The other parameters are set as $\Omega = -\xi, N = 6, \phi = \pi$ in (a,b) and $\Omega = -\sqrt{2}\xi, N = 12, \phi = 0$ in (c,d).

the resonators dimmer by dimmer inside the regime covered by the giant atom and the photonic intensity is homogenous in each resonator of the dimmer. This can be explained by the fact that the photon in the K th mode propagating to the left interferes with that propagating to the right which is revealed by Eq. (10). Since $\Omega/\xi = -1$ and $K = \pi/3$, there are photons at $j = 1, 2, 4$ and 5 but no photons at $j = 3$. On the contrary, for the parameter of $\Omega/\xi = -\sqrt{2}, \phi = \pi, N = 12$, we will reach a trimerised BIC as shown in Fig. 2 (d). It shows that in each of the trimmer, the photonic intensity in the central resonator is two times larger than those in the side ones. In this case $K = \pi/4$, so there is no photon distribution between the two legs of the giant atom at $j = 4m$ ($m = 0, 1, 2, 3$) as is demonstrated in Eq. (10). Therefore, the frequency and the photonic distribution of the BIC can be modulated by the size and the frequency of the giant atom as well as its coupling phase to the waveguide.

Besides the above mentioned BIC, in Figs. 2 (a) and (c), we can also observe a pair of BOCs, locating below and above the continuum asymmetrically, which is different from that in the resonant case ($\Omega = \omega_c$). Together with the BIC, the system exhibit an exotic dynamical behavior for both of the atom and the photonic evolution.

IV. DYNAMICS

In this section, we will investigate the dynamics of the system for both of the atomic and photonic counterpart under the parameter of $\Omega = -\xi, N = 6, \phi = \pi$, in which case the energy spectrum is given in Fig. 2(a). We set the initial state as $|\psi(0)\rangle = \sigma_+|G\rangle$, in which the giant

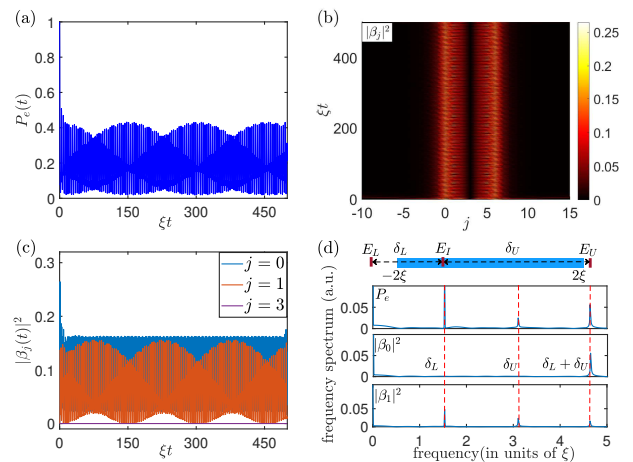


FIG. 3. The dynamical evolution of the system. (a) The dynamics of the atomic population in its excited states. (b,c) The dynamics of the photonic distribution. (d) The frequency spectrum of the atomic and photonic dynamical evolution which we obtained by the numerical Fourier transformation from the time domain to the frequency domain. The parameters are set as $\omega_c = 0, \Omega = -\xi, g = 1.1\xi, N = 6, \phi = \pi$.

atom is in its excited state while all of the resonators are in their ground states. In Fig. 3, we numerically illustrate the dynamical evolution of the system, which is governed by $|\psi(t)\rangle = \exp(-iHt)|\psi(0)\rangle$. In Fig. 3(a), we show the atomic excitation $P_e = |\langle\psi(t)|e\rangle|^2$, we can observe the slow variable envelope and the fast oscillation in each of the envelope. The dynamics of the photonic counterpart $\beta_j = \langle\psi(t)|a_j^\dagger|G\rangle$ is shown in Fig. 3(b). We can observe that the photon emitted by the giant atom is nearly completely trapped inside the covered regime. We further detailed plot the evolution of the photonic distribution in the resonator $j = 0, 1, 3$ in Fig. 3(c). We observe that the photon can never be excited in the 3th resonator, that is $|\beta_3| = 0$ during the time evolution. For $j = 1$, we find the similar quantum beats phenomenon with the atomic dynamics and the same result for $j = 2$ is not shown in the figure. For $j = 0$, we can observe a single high oscillation frequency.

To understand the above dynamical evolution, we write the initial state as

$$|\psi(0)\rangle \simeq c_U|\phi_U\rangle + c_I|\phi_I\rangle + c_L|\phi_L\rangle + \sum_k c_k|\phi_k\rangle, \quad (11)$$

where $|\phi_U\rangle$ and $|\phi_L\rangle$ are the upper and lower BOC with eigen energy E_U and E_L respectively, and $|\phi_I\rangle$ is the BIC with eigenenergy E_I . $|\phi_k\rangle$ is the k th propagating photonic mode in the waveguide, and the C-numbers c_m ($m = U, I, L, k$) denote the corresponding amplitudes. Extracting from the exact numerical results in Fig. 2(a), the eigen energy of the system is illustrated in the cartoon figure in the upper panel Fig. 3(d). Here, the continual band, which locates in the regime of $[-2\xi, 2\xi]$ by setting $\omega_c = 0$, is demonstrated by the blue bar, and the BIC and the BOCs are represented by the dark red bar.

Since the propagating modes will not contribute to the atomic dynamics when the evolution time is long enough. Therefore, in the long time limit, we will have

$$P_e(t) = |e^{-iE_L t} c_L^2 + e^{-iE_I t} c_I^2 + e^{-iE_U t} c_U^2|^2$$

$$= |e^{i\delta_L t} c_L^2 + c_I^2 + e^{-i\delta_U t} c_U^2|^2, \quad (12)$$

$$|\beta_j(t)|^2 = |e^{-i\delta_U t} c_U d_{U,j} + e^{i\delta_L t} c_L d_{L,j} + c_I d_{I,j}|^2 \quad (13)$$

where $\delta_L = E_I - E_L$ and $\delta_U = E_U - E_I$ are the detunings between of BOCs and the BIC, and $d_{\alpha,j} = \langle \phi_\alpha | a_j^\dagger | G \rangle$ ($\alpha = U, I, L$) denotes the photonic excitation amplitude on the j th resonator of the waveguide when the system is in the bound state $|\phi_\alpha\rangle$.

To further investigate the dynamical property of the system, we apply the numerical fast Fourier transformation technique to obtain the frequency spectrum for P_e and $|\beta_j|$ ($j = 0, 1$) in the lower panels of Fig. 3(d). We can observe three significant peaks for P_e and $|\beta_1|$, which locate at the frequency δ_L , δ_U and $\delta_U + \delta_L$, agreeing the analytical expression in Eq. (12). It implies that the dynamics of the giant atom is induced by the oscillations between the single BIC and the two BOCs (which contributes the peaks located at δ_U and δ_L) and between the two BOCs (which contributes the peaks located at $\delta_U + \delta_L$). On the contrary, we only find a single peak which locates at the frequency of $\delta_U + \delta_L$ in the results of $|\beta_0|$. This can also be explained by the analytical expression in Eq. (13), in which $d_{I,0} = 0$ [see Fig. 2(b)], and there only exists a single non-zero frequency component at $\delta_U + \delta_L$. It further indicates that the oscillation between the two BOCs contributes to the photonic dynamics in the zeroth cavity.

V. CONCLUSIONS

In this paper, we have investigate the possibility of control the photonic distribution in the BIC in a giant atom waveguide QED system. The BIC-BOC oscillation leads to the quantum beats dynamics. The giant atom can be realized by the superconducting transmon qubit, and the coupled resonator waveguide up to tens of sites [42, 43] and has also been fabricated in superconducting circuits. In these experimental realizations, the parameters can be achieved in the regime of $g \ll \xi \approx 100 - 200$ MHz, and therefore our predicted dynamical behavior can be observed even the giant atom suffers the spontaneous emission with the the life time of $T_1 = 10\mu\text{s}$ [44].

Beyond the specific setting considered in this work, our investigate can be develop to the system consist of more giant atoms or one giant atom which couples to the waveguide via more than one sites with the on-demand coupling strengths and phases. In these more complicated setups, the BIC and BOC is deserved to be investigated and is hopefully to design the needed dynamical process for quantum information processing.

ACKNOWLEDGMENTS

This work is supported by the funding from Jilin Province (Grant Nos. 20230101357JC and 20220502002GH) and the National Science Foundation of China (Grant No. 12375010).

Appendix A: Bound state in the continuum

In Eqs. (7) and (10), we have given the transcendental equations for the energies of the bound states and the wave function of the BIC. Here, we give a detailed derivation by transforming to momentum space.

We begin the Hamiltonian in Eq. (4), and the wave function in Eq. (6), the Schödinger equation $H|\phi\rangle = E|\phi\rangle$ yields

$$\alpha(E - \Omega) = \frac{g}{\sqrt{N_c}} \sum_k \beta_k [1 + e^{-i(kN + \phi)}],$$

$$\alpha(E - \omega_c + 2\xi \cos k) \beta_k = \frac{g}{\sqrt{N_c}} [1 + e^{i(kN + \phi)}] \quad (A1)$$

By eliminating α and β_k , the equation satisfied by E can be obtained.

$$E = \Omega + \frac{g^2}{\pi} \int_{-\pi}^{\pi} \frac{1 + \cos(kN + \phi)}{E - \omega_c + 2\xi \cos k} dk, \quad (A2)$$

which is Eq. (7) in the main text.

Next, we will prove that $E = \Omega$ is a solution of the above transcendental equation, that is to prove

$$M = \int_{-\pi}^{\pi} \frac{1 + \cos(kN + \phi)}{\Omega - \omega_c + 2\xi \cos k} dk \quad (A3)$$

is always zero. To this end, we rewrite M as

$$M = \int_{-\pi}^{\pi} \frac{1 + \cos(kN + \phi)}{\Omega - \omega_c + 2\xi \cos k} dk$$

$$= \frac{1}{2} \int_{-\pi}^{\pi} \frac{2 + e^{i(kN + \phi)} + e^{-i(kN + \phi)}}{\Delta + \xi(e^{ik} + e^{-ik})} dk$$

$$= \frac{1}{2\xi i} \oint_{|z| < 1} \frac{2z^N + z^{2N} e^{i\phi} + e^{-i\phi}}{(z - z_1)(z - z_2)z^N} dz, \quad (A4)$$

where $\Delta = \Omega - \omega_c$ and $z_{1,2} = -(\Delta/2\xi) \pm i\sqrt{1 - (\Delta/2\xi)^2} = e^{\pm iK}$ which satisfies $|z_{1,2}| = 1$. Applying the residue theorem to solve the above integral, only the N -order singular points ($z = 0$) is needed to be considered. Therefore,

$$M = \frac{\pi}{\xi} \frac{1}{(N-1)!} \frac{d^{N-1}}{dz^{N-1}} \left[\frac{2z^N + z^{2N} e^{i\phi} + e^{-i\phi}}{(z - z_1)(z - z_2)} \right]_{z=0}$$

$$= \frac{\pi e^{-i\phi}}{2i\xi \sqrt{1 - (\Delta/2\xi)^2}} (z_2^{-N} - z_1^{-N})$$

$$= \frac{\pi}{2i\xi \sqrt{1 - (\Delta/2\xi)^2}} (e^{-i(KN + \phi)} - e^{i(KN - \phi)})$$

$$= 0, \quad (A5)$$

where we have used the condition $G(K) = G(-K) = 0$ for the BIC.

From Eq. (A1), we will have

$$\frac{\beta_k}{\alpha} = \frac{g}{\sqrt{N_c}} \frac{1 + e^{i(kN+\phi)}}{E - \omega_c + 2\xi \cos k}. \quad (\text{A6})$$

Going back into the real space, we will have

$$\begin{aligned} \frac{\beta_j}{\alpha} &= \frac{g}{2\pi} \int_{-\pi}^{\pi} \frac{[1 + e^{i(kN+\phi)}]e^{-ikj}}{\Omega - \omega_c + 2\xi \cos k} dk \\ &= \frac{g}{2i\pi\xi} \oint_{|z|<1} \frac{1 + z^N e^{i\phi}}{(z - z_1)(z - z_2)z^j} dz. \end{aligned} \quad (\text{A7})$$

When $j < 0$, there is no singular point in the integral domain, so

$$\frac{\beta_j}{\alpha} = \frac{g}{2i\pi\xi} \oint_{|z|<1} \frac{1 + z^N e^{i\phi}}{(z - z_1)(z - z_2)z^j} dz = 0. \quad (\text{A8})$$

When $0 \leq j \leq N$,

$$\oint_{|z|<1} \frac{z^N e^{i\phi}}{(z - z_1)(z - z_2)z^j} dz = 0. \quad (\text{A9})$$

Therefore, we will achieve

$$\begin{aligned} \frac{\beta_j}{\alpha} &= \frac{g}{2i\pi\xi} \oint_{|z|<1} \frac{1}{(z - z_1)(z - z_2)z^j} dz \\ &= \frac{g}{\xi(j-1)!} \frac{d^{j-1}}{dz^{j-1}} \left[\frac{1}{(z - z_1)(z - z_2)} \right] \Big|_{z=0} \\ &= \frac{g}{2i\xi\sqrt{1 - (\Delta/2\xi)^2}} (z_1^j - z_2^j) \\ &= \frac{g}{2i\xi\sqrt{1 - (\Delta/2\xi)^2}} (e^{iKj} - e^{-iKj}) \\ &= \frac{g \sin(Kj)}{\xi\sqrt{1 - (\Delta/2\xi)^2}}. \end{aligned} \quad (\text{A10})$$

When $j > N$

$$\begin{aligned} \frac{\beta_j}{\alpha} &= \frac{g}{\xi(j-1)!} \frac{d^{j-1}}{dz^{j-1}} \left[\frac{1}{(z - z_1)(z - z_2)} \right] \Big|_{z=0} \\ &\quad + \frac{g}{\xi(j-N-1)!} \frac{d^{j-N-1}}{dz^{j-N-1}} \left[\frac{e^{i\phi}}{(z - z_1)(z - z_2)} \right] \Big|_{z=0} \\ &= \frac{g}{2i\xi\sqrt{1 - (\Delta/2\xi)^2}} (z_2^{-j} - z_1^{-j} + z_2^{-(j-N)} - z_1^{-(j-N)}) \\ &= \frac{ge^{iKj}}{2i\xi\sqrt{1 - (\Delta/2\xi)^2}} (1 + e^{i(KN+\phi)}) \\ &\quad - \frac{ge^{-iKj}}{2i\xi\sqrt{1 - (\Delta/2\xi)^2}} (1 + e^{i(-KN+\phi)}) \\ &= 0. \end{aligned} \quad (\text{A11})$$

Up to now, we obtain the photonic distribution in BIC which is given in Eq. (10) in the main text.

-
- [1] F. H. Stillinger, and D. R. Herrick, Bound states in the continuum, *Phys. Rev. A* **11**, 446 (1975).
- [2] D. C. Marinica, A. G. Borisov, and S. V. Shabanov, Bound States in the Continuum in Photonics, *Phys. Rev. Lett.* **100**, 183902 (2008).
- [3] M. I. Molina, A. E. Miroschnichenko, and Y. S. Kivshar, Surface Bound States in the Continuum, *Phys. Rev. Lett.* **108**, 070401 (2012).
- [4] M. Kang, T. Liu, C. T. Chan, and M. Xiao, Applications of bound states in the continuum in photonics, *Nat. Rev. Phys.* **5**, 659 (2023).
- [5] S. I. Azzam, and A. V. Kildishev, Photonic bound states in the continuum: from basics to applications, *Advanced Optical Materials* **9**, 2001469 (2021).
- [6] Y. Yu, A. Sakanas, A. R. Zali, E. Semenova, K. Yvind, and J. Mørk, Ultra-coherent Fano laser based on a bound state in the continuum, *Nat. Photon.* **15**, 758 (2021).
- [7] A. Kodigala, T. Lepetit, Q. Gu, B. Bahari, Y. Fainman, and B. Kanté, Lasing action from photonic bound states in continuum, *Nature* **541**, 196 (2017).
- [8] M. Hwang, H. Lee, K. Kim, K. Jeong, S. Kwon, K. Koshelev, Y. Kivshar, and H. Park, Ultralow-threshold laser using super-bound states in the continuum, *Nat. Commun.* **12**, 4135 (2021).
- [9] L. Carletti, K. Koshelev, C. D. Angelis, and Y. Kivshar, Giant nonlinear response at the nanoscale driven by bound states in the continuum, *Phys. Rev. Lett.* **121**, 033903 (2018).
- [10] Z. Liu, Y. Xu, Y. Lin, J. Xiang, T. Feng, Q. Cao, J. Li, S. Lan, and J. Liu, High-Q quasibound states in the continuum for nonlinear metasurfaces, *Phys. Rev. Lett.* **123**, 253901 (2019).
- [11] S. Romano, G. Zito, S. Torino, G. Calafiore, E. Penzo, G. Coppola, S. Cabrini, I. Rendina, and V. Mocella, Label-free sensing of ultralow-weight molecules with all-dielectric metasurfaces supporting bound states in the continuum, *Photon. Res.* **6**, 726 (2018).
- [12] S. Romano, G. Zito, S. N. Lara Yépez, S. Cabrini, E. Penzo, G. Coppola, I. Rendina, and V. Mocella, Tuning the exponential sensitivity of a bound-state-in-continuum optical sensor, *Opt. Express* **27**, 18776 (2019).
- [13] Z. Yu, Y. Tong, H. K. Tsang, and X. Sun, High-dimensional communication on etchless lithium niobate platform with photonic bound states in the continuum, *Nat. Commun.* **11**, 2602 (2020).
- [14] Z. Yu, and X. Sun, Acousto-optic modulation of photonic bound state in the continuum, *Light Sci. Appl.* **9**, 1 (2020).

- [15] I. Benea-Chelmsu, S. Mason, M. L. Meretska, D. L. Elder, D. Kazakov, A. Shams-Ansari, L. R. Dalton, and F. Capasso, Gigahertz free-space electro-optic modulators based on Mie resonances, *Nat. Commun.* **13**, 3170 (2022).
- [16] H. Zhang, S. Liu, Z. Guo, S. Hu, Y. Chen, Y. Li, Y. Li, and H. Chen, Topological bound state in the continuum induced unidirectional acoustic perfect absorption, *Sci. China-Phys. Mech. Astron.* **66**, 284311 (2023).
- [17] C. Chen, C.-J. Yang, and J.-H. An, Exact decoherence-free state of two distant quantum systems in a non-Markovian environment, *Phys. Rev. A* **93**, 062122 (2016).
- [18] M. V. Gustafsson, T. Aref, A. F. Kockum, M. K. Ekström, G. Johansson, and P. Delsing, Propagating phonons coupled to an artificial atom, *Science* **346**, 207 (2014).
- [19] G. Andersson, B. Suri, L. Guo, T. Aref, and P. Delsing, Non-exponential decay of a giant artificial atom, *Nat. Phys.* **15**, 1123 (2019).
- [20] B. Kannan, M. J. Ruckriegel, D. L. Campbell, A. F. Kockum, J. Braumüller, D. K. Kim, M. Kjaergaard, P. Krantz, A. Melville, B. M. Niedzielski, A. Vepsäläinen, R. Winik, J. L. Yoder, F. Nori, T. P. Orlando, S. Gustavsson, and W. D. Oliver, Waveguide quantum electrodynamics with superconducting artificial giant atoms, *Nature* **583**, 775 (2020).
- [21] A. M. Vadiraj, A. Ask, T. G. McConkey, I. Nsanzineza, C. W. Sandbo Chang, A. F. Kockum, and C. M. Wilson, Engineering the level structure of a giant artificial atom in waveguide quantum electrodynamics, *Phys. Rev. A*, **103**, 023710 (2021).
- [22] Z.-Q. Wang, Y.-P. Wang, J. Yao, R.-C. Shen, W.-J. Wu, J. Qian, J. Li, S.-Y. Zhu, and J. Q. You, Giant spin ensembles in waveguide magnonics, *Nat. Commun.* **13**, 7580 (2022).
- [23] L. Guo, A. F. Kockum, F. Marquardt, and G. Johansson, Oscillating bound states for a giant atom, *Phys. Rev. Research* **2**, 043014 (2020).
- [24] C. A. González-Gutiérrez, J. Román-Roche, and D. Zueco, Distant emitters in ultrastrong waveguide QED: Ground-state properties and non-Markovian dynamics, *Phys. Rev. A* **104**, 053701 (2021).
- [25] A. F. Kockum, G. Johansson and F. Nori, Decoherence-free interaction between giant atoms in waveguide quantum electrodynamics, *Phys. Rev. Lett.* **120**, 140404 (2018).
- [26] A. Carollo, D. Cilluffo and F. Ciccarello, Mechanism of decoherence-free coupling between giant atoms, *Phys. Rev. Research* **2**, 043184 (2020).
- [27] W. Cheng, Z. Wang, and Y.-X. Liu, Topology and retardation effect of a giant atom in a topological waveguide, *Phys. Rev. A* **106**, 033522 (2022).
- [28] L. Guo, A. Grimsmo, A. F. Kockum, M. Pletyukhov, and G. Johansson, Giant acoustic atom: A single quantum system with a deterministic time delay, *Phys. Rev. A* **95**, 053821 (2017).
- [29] A. F. Kockum, P. Delsing, and G. Johansson, Designing frequency-dependent relaxation rates and Lamb shifts for a giant artificial atom, *Phys. Rev. A* **90**, 013837 (2014).
- [30] X. Wang, T. Liu, A. F. Kockum, H.-R. Li, and F. Nori, Tunable chiral bound states with giant atoms, *Phys. Rev. Lett.* **126**, 043602 (2021).
- [31] X. Wang, Z.-M. Gao, J.-Q. Li, H.-B. Zhu, and H.-R. Li, Unconventional quantum electrodynamics with a Hofstadter-ladder waveguide, *Phys. Rev. A* **106**, 043703 (2022).
- [32] A. Soro, and A. F. Kockum, Chiral quantum optics with giant atoms, *Phys. Rev. A* **105**, 023712 (2022).
- [33] D. Wang, C. Zhao, Y. Yan, J. Yang, Z. Wang, and L. Zhou, Topology-dependent giant-atom interaction in a topological waveguide QED system, *Phys. Rev. A* **93**, 062122 (2024).
- [34] L. Leonforte, A. Carollo, and F. Ciccarello, Vacancy like Dressed States in Topological Waveguide QED, *Phys. Rev. Lett.* **126**, 063601 (2021).
- [35] W. Zhao, T. Tian, and Z. Wang, Single-photon scattering and bound states in a one-dimensional waveguide with topological giant atom, arXiv: 2401. 02104 (2024).
- [36] Q. Qiu, Y. Wu, and X. Lü, Collective Radiance of Giant Atoms in Non-Markovian Regime, *Sci. China Phys. Mech. Astron.* **66**, 224212 (2023).
- [37] K. H. Lim, W. Mok, and L. Kwek, Oscillating bound states in non-Markovian photonic lattices, *Phys. Rev. A* **107**, 023716 (2023).
- [38] X. Zhang, C. Liu, Z. Gong, and Z. Wang, Quantum interference and controllable magic cavity QED via a giant atom in a coupled resonator waveguide, *Phys. Rev. A* **108**, 013704 (2023).
- [39] G. Calajó, F. Ciccarello, D. Chang, and P. Rabl, Atom-field dressed states in slow-light waveguide QED, *Phys. Rev. A* **93**, 033833 (2016).
- [40] L. Zhou, H. Dong, Y. Liu, C. P. Sun, and F. Nori, Quantum supercavity with atomic mirrors, *Phys. Rev. A* **78**, 063827 (2008).
- [41] L. Qiao, Y.-J. Song, and C.-P. Sun, Quantum phase transition and interference trapping of populations in a coupled-resonator waveguide, *Phys. Rev. A* **100**, 013825 (2021).
- [42] M. Scigliuzzo, G. Calajò, F. Ciccarello, D. P. Lozano, A. Bengtsson, P. Scarlino, A. Wallraff, D. Chang, P. Delsing, and S. Gasparinetti, Controlling Atom-Photon Bound States in an Array of Josephson-Junction Resonators, *Phys. Rev. X* **12**, 031036 (2022).
- [43] X. Zhang, E. Kim, D. K. Mark, S. Choi, and O. Painter, A superconducting quantum simulator based on a photonic-bandgap metamaterial, *Science* **379**, 278 (2023).
- [44] M. Kjaergaard, M.E. Schwartz, J. Braumüller, P. Krantz, J. I.-J. Wang, S. Gustavsson, and W. D. Oliver, *Annu. Rev. Condens. Matter Phys.* **11**, 369 (2020).